Supplemental material for "Global impacts of subseasonal wind variability on ocean surface stress, buoyancy flux, and mixed layer depth"

D. B. Whitt[1], S. A. Nicholson[2], and M. M. Carranza[1]

1. Contents of this file

Figures S1 to S8.

2. Validating the CTL simulation

This supplementary text reports on a validation analysis that compares the model output against in situ observations.

Several previous studies have validated mesoscale-resolving CESM model solutions/configurations that are similar to the CTL experiment by comparing the model

Corresponding author: D. B. Whitt, National Center for Atmospheric Research, PO Box 3000, Boulder, CO 80307 (dwhitt@ucar.edu)

[1]National Center for Atmospheric Research, Boulder, CO, USA.

[2]Southern Ocean Carbon-Climate Observatory (SOCCO), CSIR, Cape Town, South Africa

results to independent observations [*Bryan and Bachman*, 2015; *Johnson et al.*, 2016; *Harrison et al.*, 2018; *DuVivier et al.*, 2018; *Delman et al.*, 2018]. Here, we discuss a few new comparisons that demonstrate the model's ability to simulate the observed climatological MLD in the CTL experiment (as well as its deficiencies in this regard). Unlike previous validation efforts, we compare against observations using *in situ* profile data and the same MLD definition for the observations and model data (i.e., as computed in the model, and described in *Large et al.* [1997], page 2427). In-situ profile data of temperature, and salinity are converted to conservative temperature and absolute salinity, from which density is derived using the international thermodynamic equation of seawater (TEOS-10, [*McDougall and Barker*, 2011]). Quality-controlled instantaneous profile data from the Coriolis Ocean Dataset for Reanalysis (CORA v5.1, [*Cabanes et al.*, 2013], available at http://marine.copernicus.eu/services-portfolio/access-to-products/) collected between January 2000 and December 2017 are used for the analyses. The MLD is calculated for each profile, after the density is linearly interpolated to a uniform grid with 5 m resolution and then smoothed with a 15 point (75 m) moving average. Some smoothing of the observed density profiles is necessary in order to make meaningful global comparisons between the model and observations. In particular, the observed MLD is highly sensitive to the smoothing in crucial regions where the MLD is deep and the stratification is weak (e.g., the Labrador Sea during winter). However, the MLD is not particularly sensitive to either the definition or the smoothing procedure over most of the ocean most of the time. For example, Figure S7 compares the annual mean MLD calculated with this *Large et al.* [1997] method and the algorithm proposed by *Holte et al.* [2017] as well as the MLD defined by a 0.03 kg/m^3 density threshold [*de Boyer Montégut et al.*, 2004]. The definition used here produces a climatological mean MLD that is mostly (although not everywhere) somewhat deeper than these other two definitions.

Monthly climatologies of MLD, sea surface temperature (SST) and sea surface salinity (SSS) for the top 10 m are constructed by bin-averaging profile data in 2° bins for each month, and model output was regridded to the same regular grid for comparisons against observations. Significance for the differences between model and observations was evaluated by means of a bootstrap method over 100 realizations, and a confidence level of 95%, assuming all observed profiles are independent.

Biases in climatological mean surface temperature and salinity relative to observations are almost everywhere less than 3°C and 1 g kg^{-1} but mostly smaller (Figure S2). There are notable cold surface temperature biases in the model in the Irminger and Norwegian Seas, as well as in the vicinity of the northwest corner of the North Atlantic Current (east of Newfoundland). Notable warm surface temperature biases are observed on the eastern boundaries of North and South Pacific as well the western margin of the subtropical North Atlantic (north of Cape Hatteras) and subtropical North Pacific, including much of seaward extension of the Kuroshio, and the Southern Ocean. The modeled global ocean surface salinity is mostly fresher than the climatology from observations, particularly at mid-to-high latitudes [similar to a previous low-resolution CESM, see *Griffies et al.*, 2009]. However, there is a notable fresh bias in the vicinity of the northwest corner of the North Atlantic Current. Notable salty biases are observed in the western tropical North Atlantic and along a thin strip just north of the equator that extends seaward from the eastern boundaries of the Atlantic and Pacific. On a global scale, the magnitudes of these biases are generally comparable to or smaller than the magnitude of the biases observed in 500-

year simulations on a grid with nominal 1° resolution with the same CORE-1 forcing protocol [*Griffies et al.*, 2009].

Model MLDs are also qualitatively similar to observed MLDs, although there are important differences (Figure S3). For example, simulated mean mixed layers are generally deepest in the observed sites of deep mixing and winter watermass formation, including a narrow deep mixing band in the Sub-Antarctic zone of the Southern Ocean, the subpolar North Atlantic including the Labrador Sea, above the Greenland-Iceland-Faroe Ridge complex, and parts of the Norwegian and Barents Seas. Biases are small during late summer, but modeled MLDs are almost universally slightly shallower than observed during that season. Notable biases include annual mean MLDs that are too deep in the modeled central to eastern tropical Pacific compared to observations (Figure S3). Conversely, hot spots of deep winter MLDs are almost universally too shallow in the simulations, including in the subpolar North Atlantic during March. In addition, the simulated MLDs are too shallow in most of the observed deep winter mixing band in the Subantarctic Southern Ocean during September. Somewhat surprisingly, these results contrast with those of *DuVivier et al.* [2018], as there is no clear indication that modeled MLDs are too deep in any significant part of this Subantarctic deep mixing band (compare with their Figure 10). This contrast highlights the rather strong and qualitative sensitivity of MLD biases to the chosen definition of the MLD and its precise construction in crucial regions of deep MLD and watermass formation.

It may be noted that there is no data to compare to in the Arctic, which is a disadvantage of using an Argo-based data set; but, the generally shallow mean of 32 m in CTL and 48 m mean difference from shallowest to deepest depth in the monthly climatology is consistent with other observations [*Peralta-Ferriz and Woodgate*, 2015]. Further, the spatial distribution of the MLD is qualitatively consistent with observations in the Arctic. Deeper mixed layers and largest seasonal cycle amplitudes are in the Barents Sea, Marakov Basin, and Eurasian Basin and shallower mixed layers and smaller seasonal cycle amplitudes are in the Canada Basin and the Chuckchi Sea (not shown).

Some of the differences between the model and observations are probably attributable to the temporal inconsistency between the atmospheric forcing data sets (1958-2000) and the MLD observations (after 2000), but presumably not all.

3. Supplemental Figures

References

Bryan, F., and S. Bachman (2015), Isohaline salinity budget of the north atlantic salinity maximum, *Journal of Physical Oceanography*, *45*(3), 724–736.

Cabanes, C., A. Grouazel, K. v. Schuckmann, M. Hamon, V. Turpin, C. Coatanoan, F. Paris, S. Guinehut, C. Boone, N. Ferry, et al. (2013), The cora dataset: validation and diagnostics of in-situ ocean temperature and salinity measurements, *Ocean Science*, *9*(1), 1–18.

de Boyer Montégut, C., G. Madec, A. S. Fischer, A. Lazar, and D. Iudicone (2004), Mixed layer depth over the global ocean: An examination of profile data and a profile-based climatology., *J. Geophys. Res.*, *109*, C12,003, doi:10.1029/2004JC002378.

Delman, A. S., J. L. McClean, J. Sprintall, L. D. Talley, and F. O. Bryan (2018), Process-specific contributions to anomalous java mixed layer cooling during positive iod events, *Journal of Geophysical Research: Oceans*, *123*(6), 4153–4176.

DuVivier, A. K., W. G. Large, and R. J. Small (2018), Argo observations of the deep mixing band in the southern ocean: A salinity modeling challenge, *Journal of Geophysical Research: Oceans*, *123*(10), 7599–7617.

Griffies, S. M., A. Biastoch, C. Böning, F. Bryan, G. Danabasoglu, E. P. Chassignet, M. H. England, R. Gerdes, H. Haak, R. W. Hallberg, et al. (2009), Coordinated ocean-ice reference experiments (cores), *Ocean modelling*, *26*(1-2), 1–46.

Harrison, C. S., M. C. Long, N. S. Lovenduski, and J. K. Moore (2018), Mesoscale effects on carbon export: a global perspective, *Global Biogeochemical Cycles*, *32*(4), 680–703.

Holte, J., L. D. Talley, J. Gilson, and D. Roemmich (2017), An argo mixed layer climatology and database, *Geophysical Research Letters*, *44*(11), 5618–5626.

Johnson, B. K., F. O. Bryan, S. A. Grodsky, and J. A. Carton (2016), Climatological annual cycle of the salinity budgets of the subtropical maxima, *Journal of Physical Oceanography*, *46*(10), 2981–2994.

Large, W. G., G. Danabasoglu, S. C. Doney, and J. C. McWilliams (1997), Sensitivity to surface forcing and boundary layer mixing in a global ocean model: Annual-mean climatology, *Journal of Physical Oceanography*, *27*(11), 2418–2447.

McDougall, T. J., and P. M. Barker (2011), Getting started with teos-10 and the gibbs seawater (gsw) oceanographic toolbox, *SCOR/IAPSO WG*, *127*, 1–28.

Peralta-Ferriz, C., and R. A. Woodgate (2015), Seasonal and interannual variability of pan-arctic surface mixed layer properties from 1979 to 2012 from hydrographic data, and the dominance of stratification for multiyear mixed layer depth shoaling, *Progress in Oceanography*, *134*, 19–53.

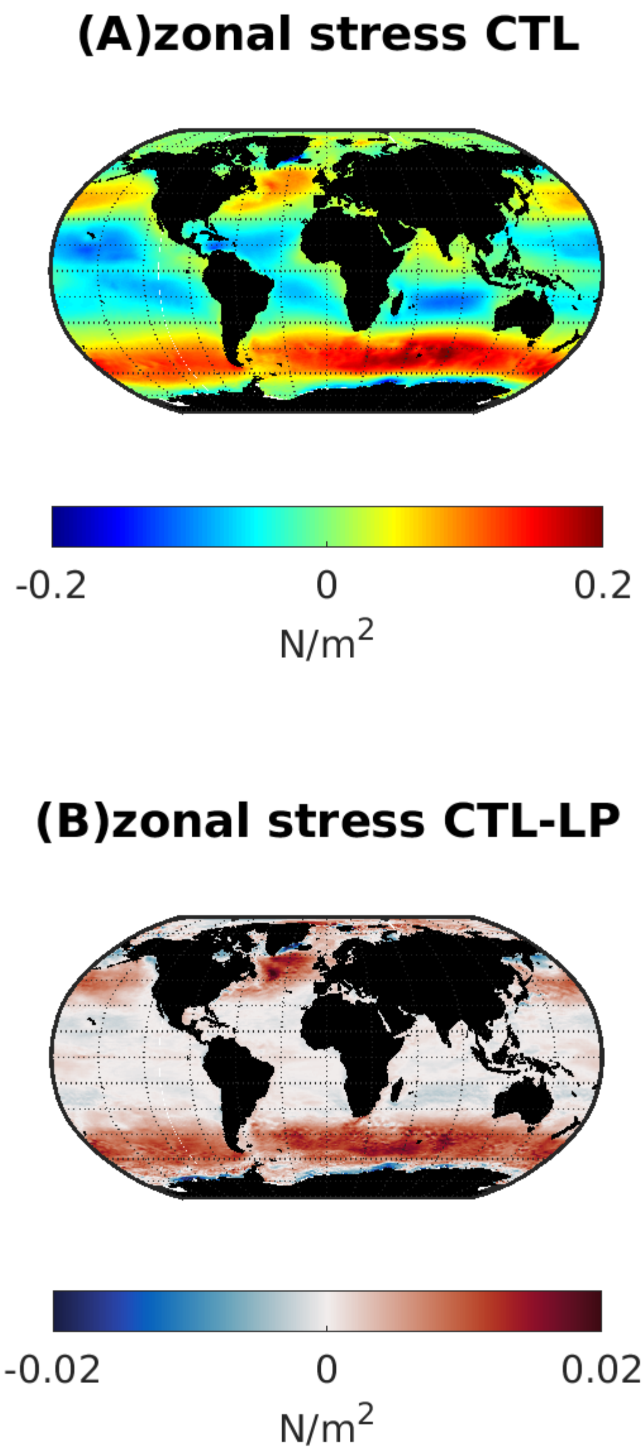

Figure S1. (a) Mean zonal stress in the CTL simulation, and (b) the difference between CTL and LP simulations.

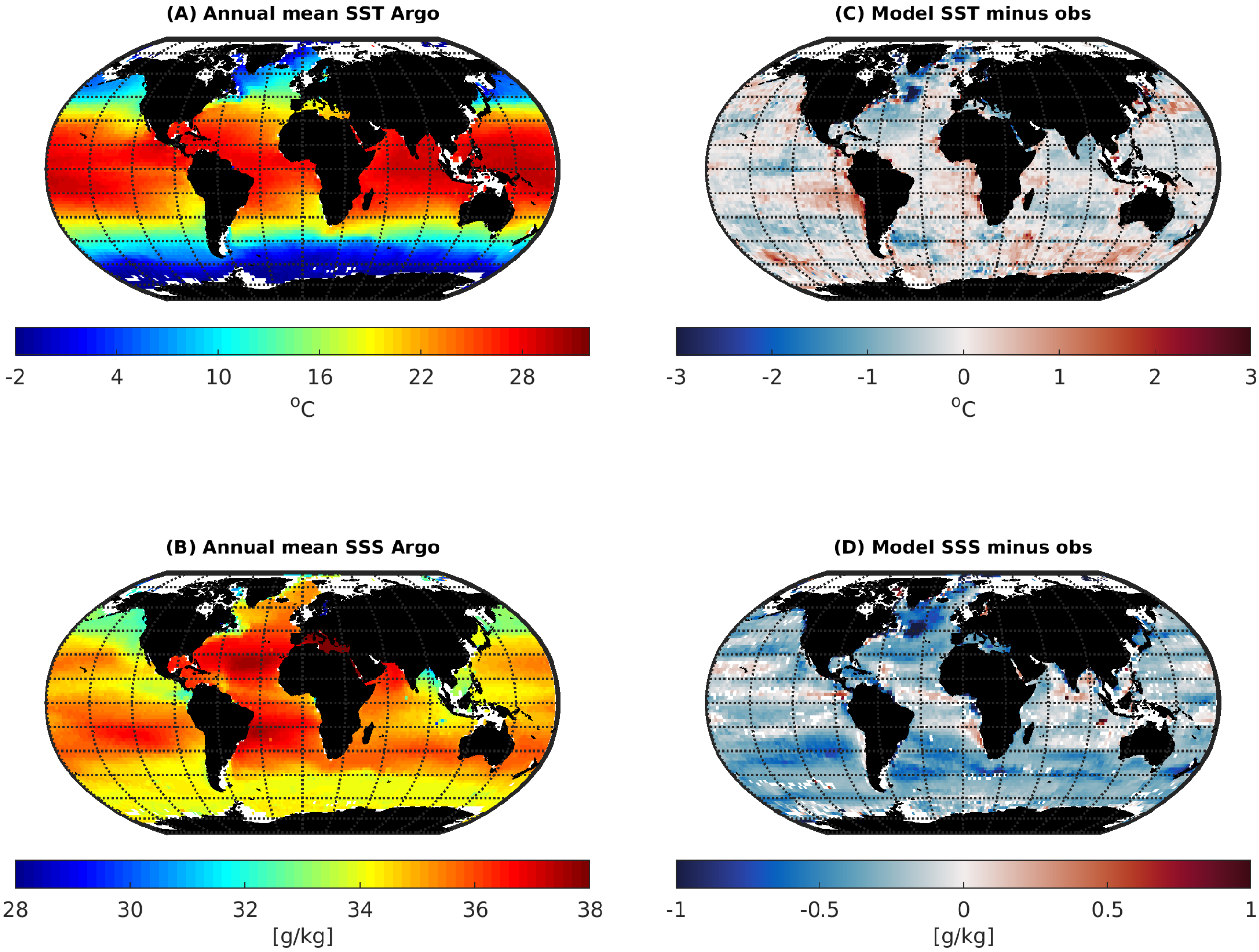

Figure S2. A comparison between the global mean temperature and salinity averaged over the top 10 m from Argo profiles computed between 2000 and 2017 and the simulated five-year time-mean temperature and salinity in the top model grid cell (0-10 m) of the CTL simulation. These results may be compared with Figures 7-8 in *Griffies et al.* [2009], where surface temperature and salinity are compared in several lower-resolution models forced by the CORE-1 normal year.

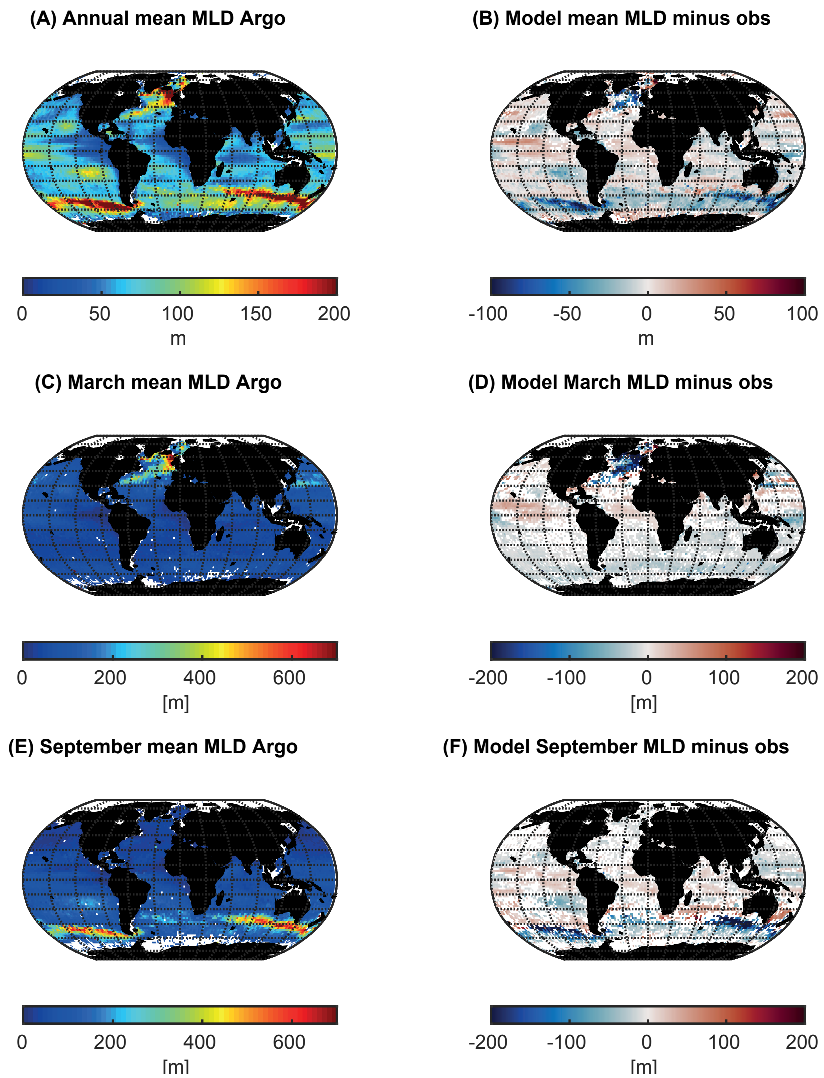

Figure S3. A comparison between the observed (Argo, 2000-2017) and simulated climatological MLD, both of which are calculated using the *Large et al.* [1997] algorithm. (Top) Annual means, (middle) March means, and (bottom) September means.

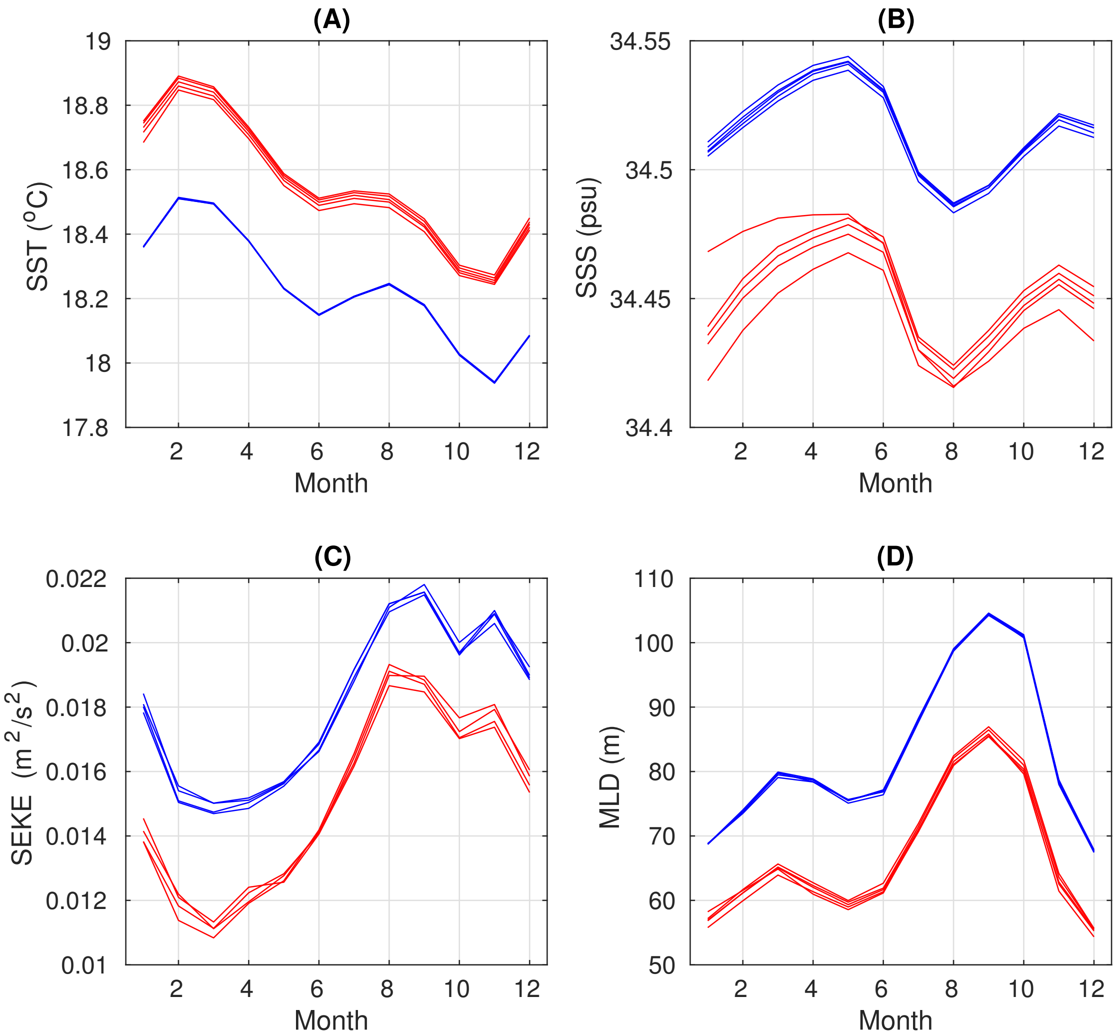

Figure S4. Time series of global mean surface temperature (A), salinity (B), a measure of surface eddy kinetic energy $SEKE = 1/2(u^2 - \langle u\rangle_t^2 + v^2 - \langle v\rangle_t^2)$ (C), and mixed layer depth (D) in the CTL (blue) and LP (red) simulations. Each line represents one of the sequential five years of each simulation. The fact that the lines are tightly clustered in each simulation demonstrates that the drift on inter-annual timescales in LP and CTL is relatively small compared to the amplitude of the seasonal cycle and the magnitude of the differences between LP and CTL. Note that there are only 4 lines for kinetic energy and in that case the time average $\langle\rangle_t$ only includes years 18-20 and 22, because the kinetic energy was not output to the monthly average files during year 21.

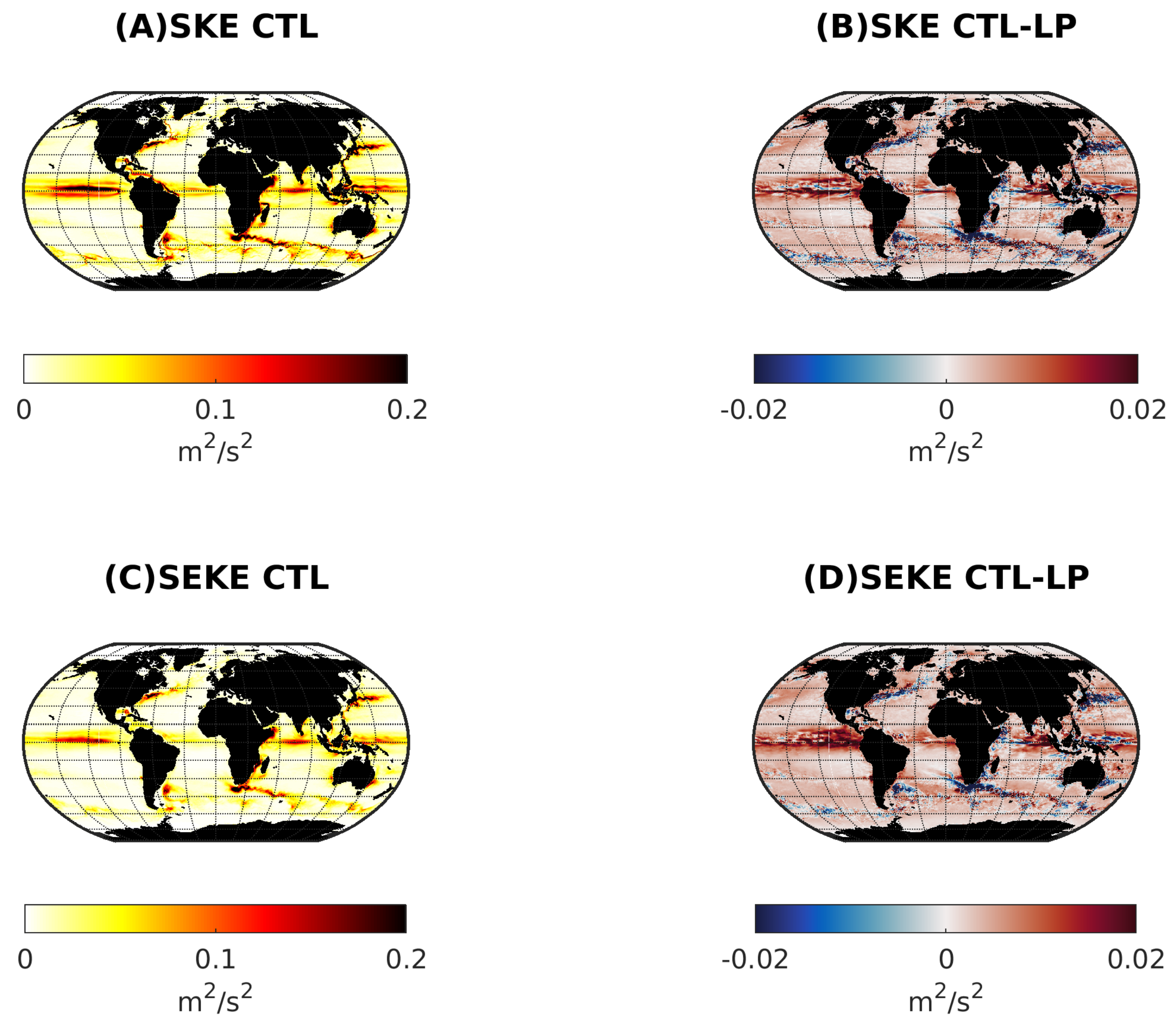

Figure S5. (a) Mean surface kinetic energy $SKE = \langle 1/2(u^2+v^2)\rangle_t$ and (c) surface eddy kinetic energy $SEKE = SKE - 1/2(\langle u\rangle_t^2 + \langle v\rangle_t^2)$ and (b)-(d) the respective differences between CTL and LP simulations. Note that the time average $\langle\rangle_t$ only includes years 18-20 and 22, because the kinetic energy was not output to the monthly average files during year 21.

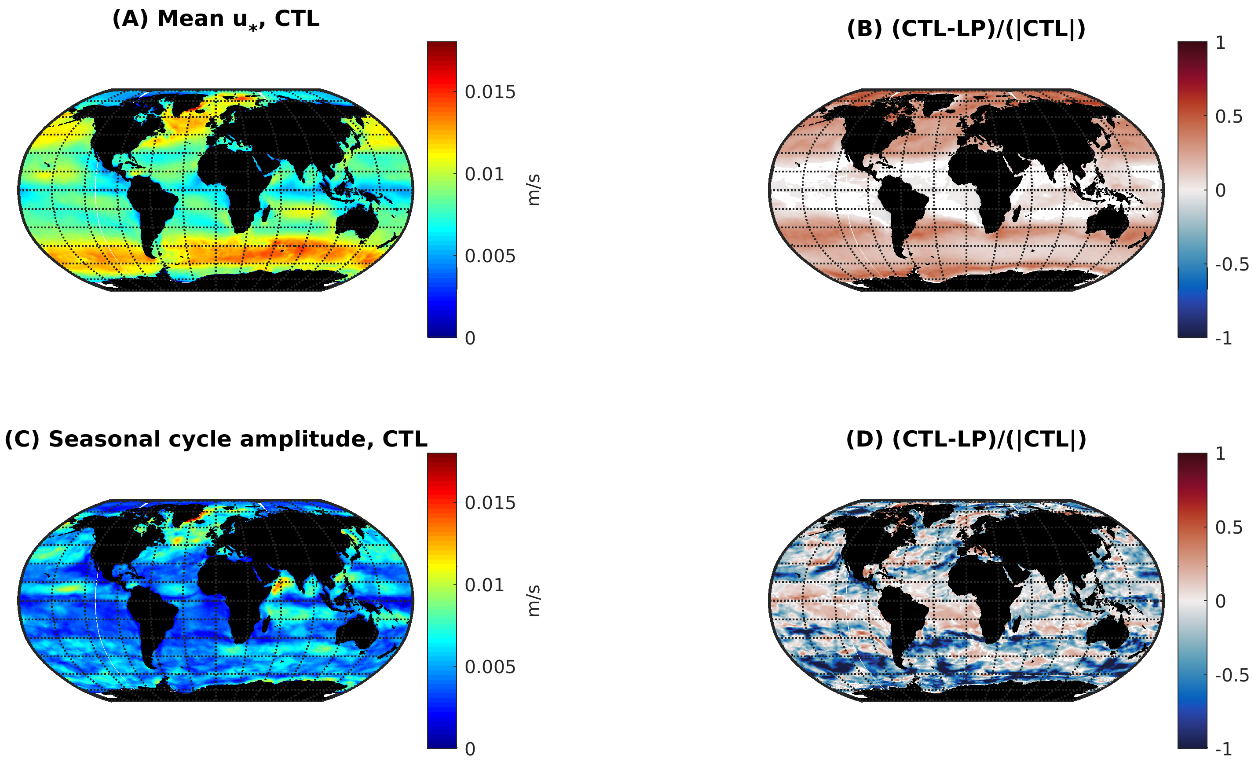

Figure S6. As in Figure 1 of the main manuscript, but friction velocity u_*.

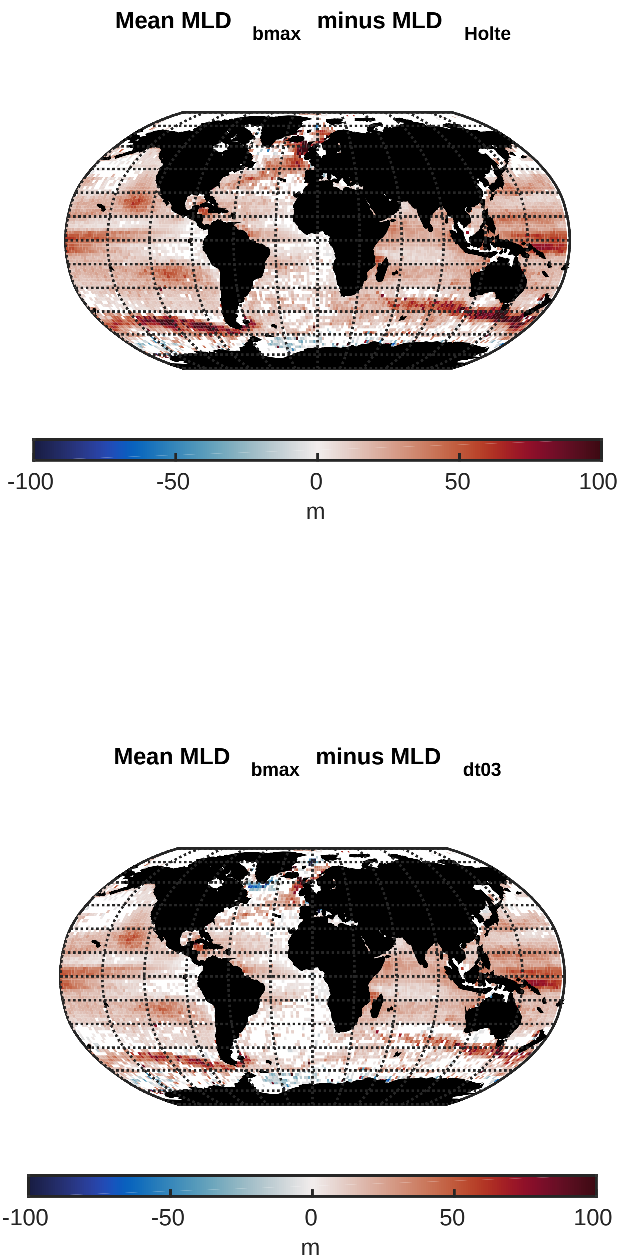

Figure S7. Differences between observed annual mean Argo MLD climatologies for different MLD definitions. Top: MLD "bmax" (as defined here and modified from *Large et al.* [1997]) and MLD "holte" [as defined in *Holte et al.*, 2017]. Bottom: MLD "bmax" minus the MLD defined by a 0.03 kg/m^3 density threshold [*de Boyer Montégut et al.*, 2004] (bottom).

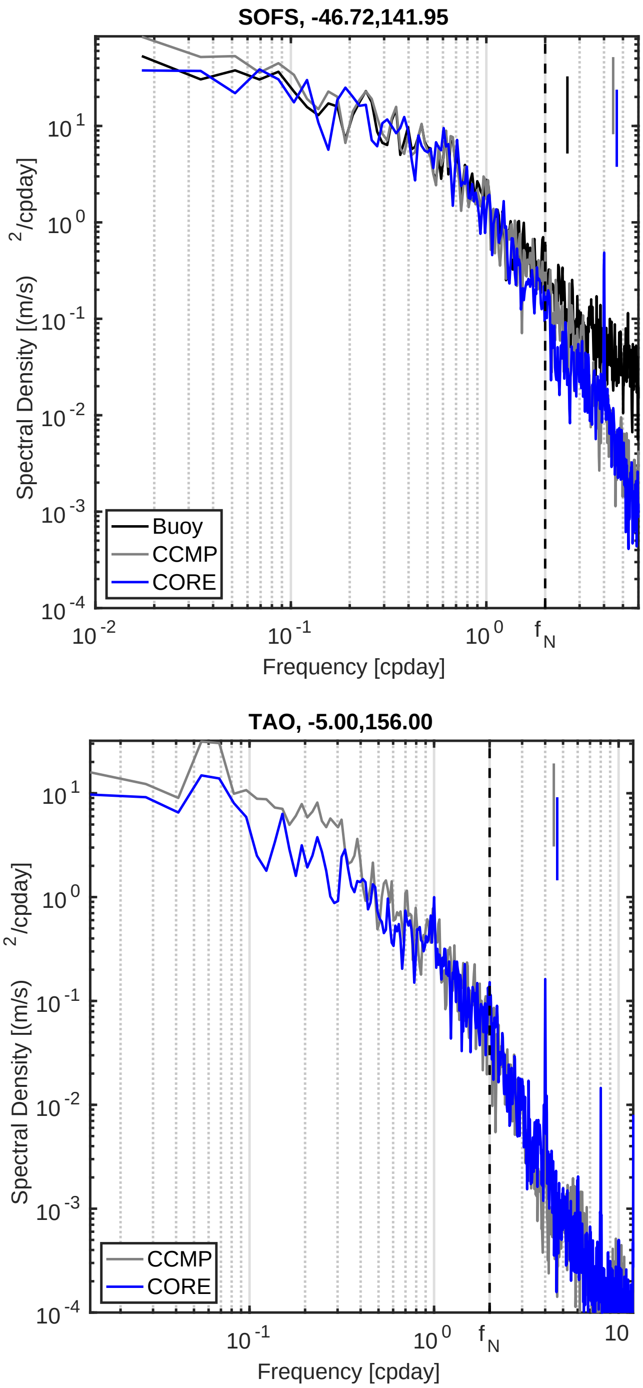

Figure S8. Some example comparisons between speed power spectra derived from the CTL winds, the CCMP satellite winds, and buoy measurements. The power spectra should not be identical because the observations are from particular years, whereas the CTL has climatological power at each frequency. The location (latitude °N, longitude °E) is as indicated in the titles. The top comparison is from the year 2010, the bottom is from the year 1995.